frontiers in Marine Science

ORIGINAL RESEARCH
published: 12 July 2019
doi: 10.3389/fmars.2019.00397

The Roles of Suspension-Feeding and Flux-Feeding Zooplankton as Gatekeepers of Particle Flux Into the Mesopelagic Ocean in the Northeast Pacific

Michael R. Stukel[1,2], Mark D. Ohman[3], Thomas B. Kelly[1] and Tristan Biard[4]*

[1] Department of Earth, Ocean, and Atmospheric Science, Florida State University, Tallahassee, FL, United States, [2] Center for Ocean-Atmospheric Prediction Studies, Florida State University, Tallahassee, FL, United States, [3] Scripps Institution of Oceanography, University of California, San Diego, San Diego, CA, United States, [4] Laboratoire d'Océanologie et de Géosciences, Wimereux, France

OPEN ACCESS

Edited by:
Rainer Kiko, GEOMAR Helmholtz Centre for Ocean Research Kiel, Germany

Reviewed by:
John Patrick Dunne, Geophysical Fluid Dynamics Laboratory (GFDL), United States
Hiroaki Saito, The University of Tokyo, Japan
Santiago Hernández-León, University of Las Palmas de Gran Canaria, Spain

***Correspondence:**
Michael R. Stukel
mstukel@fsu.edu

Specialty section:
This article was submitted to Marine Biogeochemistry, a section of the journal Frontiers in Marine Science

Received: *26 March 2019*
Accepted: *26 June 2019*
Published: *12 July 2019*

Citation:
Stukel MR, Ohman MD, Kelly TB and Biard T (2019) The Roles of Suspension-Feeding and Flux-Feeding Zooplankton as Gatekeepers of Particle Flux Into the Mesopelagic Ocean in the Northeast Pacific. Front. Mar. Sci. 6:397. doi: 10.3389/fmars.2019.00397

Zooplankton are important consumers of sinking particles in the ocean's twilight zone. However, the impact of different taxa depends on their feeding mode. In contrast to typical suspension-feeding zooplankton, flux-feeding taxa preferentially consume rapidly sinking particles that would otherwise penetrate into the deep ocean. To quantify the potential impact of two flux-feeding zooplankton taxa [Aulosphaeridae (Rhizaria), and *Limacina helicina* (euthecosome pteropod)] and the total suspension-feeding zooplankton community, we measured depth-stratified abundances of these organisms during six cruises in the California Current Ecosystem. Using allometric–scaling relationships, we computed the percentage of carbon flux intercepted by flux feeders and suspension feeders. These estimates were compared to direct measurements of carbon flux attenuation (CFA) made using drifting sediment traps and ^{238}U–^{234}Th disequilibrium. We found that CFA in the shallow twilight zone typically ranged from 500 to 1000 μmol organic C flux remineralized per 10-m vertical depth bin. This equated to approximately 6–10% of carbon flux remineralized/10 m. The two flux-feeding taxa considered in this study could account for a substantial proportion of this flux near the base of the euphotic zone. The mean flux attenuation attributable to Aulosphaeridae was 0.69%/10 m (median = 0.21%/10 m, interquartile range = 0.04–0.81%) at their depth of maximum abundance (∼100 m), which would equate to ∼10% of total flux attenuation in this depth range. The maximum flux attenuation attributable to Aulosphaeridae reached 4.2%/10 m when these protists were most abundant. *L. helicina*, meanwhile, could intercept 0.45–1.6% of carbon flux/10 m, which was slightly greater (on average) than the Aulosphaeridae. In contrast, suspension-feeding zooplankton in the mesopelagic (including copepods, euphausiids, appendicularians, and ostracods) had combined clearance rates of 2–81 L m^{-3} day^{-1} (mean of 19.6 L m^{-3} day^{-1}). This implies a substantial impact on slowly sinking particles, but

a negligible impact on the presumably rapidly sinking fecal pellets that comprised the majority of the material collected in sediment traps. Our results highlight the need for a greater research focus on the many taxa that potentially act as flux feeders in the oceanic twilight zone.

Keywords: biological pump, carbon export, remineralization length scale, mesozooplankton ecology, pteropods, marine biogeochemistry, sinking particles, marine snow

INTRODUCTION

Zooplankton play diverse roles in the cycling of many elements in the ocean including iron, zinc, sulfur, and mercury (Fowler, 1977; Asher et al., 2016; Baines et al., 2016; Schmidt et al., 2016; Gorokhova et al., 2018). However, their greatest importance to global biogeochemistry is likely derived from their roles in the biological carbon pump (BCP; Buitenhuis et al., 2006; Turner, 2015; Steinberg and Landry, 2017). The BCP refers to the processes that transport organic carbon fixed by phytoplankton in the euphotic zone into the mesopelagic realm (Silver and Gowing, 1991; Ducklow et al., 2001; Siegel et al., 2016). The BCP leads to net transport of CO_2 from the surface ocean into the deep ocean where it can be sequestered for periods of decades to millennia (DeVries et al., 2012). Estimates of the present magnitude of the BCP range from 5 to 12 Pg C year^{-1} (Henson et al., 2011; Laws et al., 2011; Siegel et al., 2014; DeVries and Weber, 2017), however, the responses of mesozooplankton and the BCP to future climate change remain unknown.

Research on the role of mesozooplankton in the BCP has focused primarily on the epipelagic zone where the relationship between zooplankton and the BCP can change based on the community composition of phytoplankton and zooplankton. Zooplankton can play an important role in combining smaller particles into large, rapidly sinking fecal pellets (Bruland and Silver, 1981; Komar et al., 1981; Turner, 2002; Wilson et al., 2008) and promote aggregation and sinking through discarded mucous feeding webs (Alldredge, 1976; Hansen et al., 1996; Robison et al., 2005). Zooplankton can also decrease the magnitude of the biological pump when their grazing activities exert top-down control on phytoplankton production (Glibert, 1998; Goericke, 2002) or fragment larger particles into smaller ones (Dilling and Alldredge, 2000), and also play an important role in nutrient regeneration in the euphotic zone (Frangoulis et al., 2005; Alcaraz et al., 2010; Saba et al., 2011). Active transport by diel vertically migrating zooplankton is also an important (potentially dominant) component of the biological pump in many marine ecosystems (Steinberg et al., 2000; Hannides et al., 2009; Bianchi et al., 2013; Stukel et al., 2018b; Archibald et al., 2019; Hernández-Leon et al., unpublished; Kelly et al., unpublished; Kiko et al., unpublished).

Although fewer studies have quantified zooplankton impacts in the mesopelagic, zooplankton play a substantial role in consuming, disaggregating, and transforming sinking particles (Steinberg and Landry, 2017). These organisms may play a substantial role in modulating marine snow flux in the mesopelagic (Lampitt et al., 1993) and have been hypothesized to play roles as "gatekeepers" that modulate carbon transfer from the euphotic zone to the mesopelagic (Jackson and Checkley, 2011). However, zooplankton are phylogenetically and functionally diverse with a wide array of feeding strategies (Kiørboe, 2011). It is thus important to consider the relative importance of zooplankton with different feeding modes. For instance, suspension-feeding salps and crustaceans may consume particles in relative proportion to their abundance in the water column, although they may show selectivity based on particle size or other characteristics (Fuchs and Franks, 2010). In contrast, a flux-feeding pteropod will intercept particles in proportion to the speed with which they sink through the water column (Jackson et al., 1993), while cruise-feeding zooplankton may search for and colonize large aggregates (Kiørboe and Thygesen, 2001). Yet other taxa may break aggregates apart due to their swimming and feeding behaviors or partially consume fecal pellets leading to breakage and decreased settling velocities (Goldthwait et al., 2004; Iversen and Poulsen, 2007). Understanding these interactions is important to understanding observed decadal scale changes in carbon flux attenuation (CFA) in the mesopelagic (Lomas et al., 2010).

In this study we investigate the relative importance of representatives of two groups of flux-feeding zooplankton (phaeodarians and euthecosome pteropods) with respect to sinking particle flux attenuation. Phaeodarians are a group of siliceous protists from the supergroup Rhizaria that typically thrive in the deep ocean (Nakamura and Suzuki, 2015). We focus in this manuscript on one group of large Phaeodaria (Aulosphaeridae) that have a typical diameter of ∼2-mm and are common in the shallow twilight zone in the CCE (Ohman et al., 2012; Biard et al., 2016, 2018). These mesopelagic phaeodarians are likely flux feeders that have relatively slow (for protists) growth rates and rely on the rain of sinking particles from above for their food (Gowing, 1986, 1989; Gowing and Bentham, 1994; Stukel et al., 2018a). Euthecosome pteropods are pelagic molluscs that produce large mucous feeding webs to trap food, including swimming zooplankton and sinking particles (Gilmer and Harbison, 1986; Lalli and Gilmer, 1989). We focus on the species *Limacina helicina*, which is common in cold waters worldwide from the Antarctic to the Arctic including the California Current (Hunt et al., 2010; Bednaršek et al., 2012). *L. helicina* produces a mucous feeding web with a typical diameter of 40–55 mm (Gilmer and Harbison, 1986). We draw our data from a decade's worth of field campaigns with differing objectives and hence changing methodology. We thus do not intend this to be a definitive assessment of the role of flux feeders in the mesopelagic ecosystem. Rather we intend it as an initial quantitative investigation of the differing roles of suspension feeders and two specific taxa of flux feeders.

We find that each of these flux feeders has the potential to mediate a substantial portion of the CFA in the shallow twilight zone, although their impact is greatly reduced in the deeper mesopelagic. In contrast, suspension-feeding zooplankton are abundant through the mesopelagic, but likely only play a substantial role in the attenuation of the flux of slowly sinking particles. There is, however, substantial uncertainty around our core conclusions, and we hope that this uncertainty will spur future targeted investigations.

MATERIALS AND METHODS

Field Sampling

In situ measurements were made on six process cruises of the CCE LTER Program (P0704, April 2007; P0810, October 2008; P1106, June 2011; P1208, August 2012; P1408, August 2014; and P1604 April 2016, **Figure 1**). On these cruises, we used a quasi-Lagrangian sampling scheme to track water parcels for a period of 2–5 days while quantifying biotic and abiotic standing stocks and rates (Landry et al., 2009, 2012). After preliminary site surveys with a free-fall Moving Vessel Profiler (Ohman et al., 2012), quasi-Lagrangian experiments (hereafter referred to as "cycles") were initiated with the deployment of a surface-tethered drifting sediment trap with a 3 × 1-m drogue centered at 15-m depth to track the mixed layer (Stukel et al., 2013). A second, identically drogued, experimental array was deployed and recovered daily while being used as a platform for *in situ* incubations (Landry et al., 2009). During each cycle, paired day–night Multiple Opening and Closing Net and Environmental Sensing System (MOCNESS) net tows were used to determine vertical patterns of mesozooplankton abundance (Powell and Ohman, 2015). On approximately 10 CTD-Niskin rosette casts per cycle, we used an Underwater Vision Profiler (UVP5) to determine vertical profiles of rhizarians (Ohman et al., 2012; Biard et al., 2018). We also measured the vertical flux (and flux attenuation) of sinking particles using the aforementioned drifting sediment traps and measurements of water column ^{238}U–^{234}Th deficiency (Stukel et al., 2015). We divided our Lagrangian experiments into oligotrophic cycles (<0.5 μg Chl a L^{-1}) or high biomass cycles (>0.5 μg Chl a L^{-1}). For details on cruise conditions, see **Supplementary Materials**.

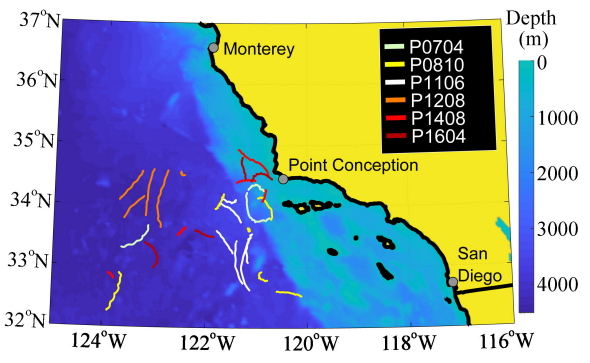

FIGURE 1 | Study region showing Lagrangian tracks of each experimental cycle (color coded by cruise). Blue shading show bathymetry.

Zooplankton Collection and Enumeration

Mesozooplankton depth-stratified abundances were determined from day–night MOCNESS tows (1 m^2 net, 202-μm mesh) on the P0704 and P0810 cruises (typically two pairs of tows per cycle). Each net collected organisms over a ∼50-m depth interval with consecutive nets tripped from a depth of 450 m to the surface. Samples were preserved in 1.8% formaldehyde and analyzed using a ZooScan digital scanner with ZooProcess software (Gorsky et al., 2010). Zooplankton were sorted into broad taxonomic groups (e.g., copepods, euphausiids, doliolids, etc.) using machine learning algorithms, the taxonomic assignments of 100% of the vignettes validated manually, then automatically sized (as Feret diameter). Organismal length was then used with allometric equations (see below) to quantify organism biomass and clearance rate. For additional details on ZooScan processing, see Stukel et al. (2013), Powell and Ohman (2015), and Ohman and Romagnan (2016). On two cycles from the P1208 cruise, these samples were also sorted to enumerate the abundance of pteropods, specifically *L. helicina* (Bednaršek and Ohman, 2015).

Because they are not well preserved in net tows, large rhizarians (>600-μm) were quantified using an UVP5 (Picheral et al., 2010; Biard et al., 2016). The UVP5 is an *in situ* imaging camera that was mounted downward facing on the bottom of the ship's CTD-Niskin rosette and deployed an average of 10 times per Lagrangian cycle. It reliably images organisms that are >600-μm in diameter, although avoidance issues should be expected for strongly swimming taxa. The UVP5 images a volume of ∼1 L per image at ∼6 Hz. Data were analyzed as described in Biard et al. (2016, 2018). Briefly, images were automatically analyzed to separate out vignettes representing organisms or marine snow aggregates. ZooProcess software was utilized to generate morphometric information (e.g., diameter) and classify the organisms into broad taxonomic groups. Classifications were then 100% manually validated. Phaeodarian taxonomic groups included Aulosphaeridae, which was the dominant rhizarian present and is the only group of organisms enumerated by UVP5 that is utilized in this study.

Sediment Trap Deployments

VERTEX-style particle interceptor tube (PIT) sediment traps were deployed at the beginning and recovered at the end of each cycle (Knauer et al., 1979; Stukel et al., 2013). PITs consisted of a polycarbonate tube with 7-cm inner diameter and 8:1 aspect ratio with a baffle on top comprised of 13 smaller, beveled tubes. On the P0704 cruise, PITs were deployed at a depth of 100 m. On P0810, P1106, and P1208, PITs were deployed at a depth of 100 m and near the base of the euphotic zone (as estimated based on fluorescence profiles from MVP transects) if the base of the euphotic zone was shallower than 75 m. On the P1408 and P1604 cruises, PITs were deployed at the base of the euphotic zone, 100 m, and 150 m.

PITs were deployed with a dense formaldehyde-filtered seawater brine. Deployments lasted from 2.25 to 4.25 days. After

recovery, the interface separating brine water from overlying ambient seawater was identified and the overlying seawater was immediately removed. Samples were then gravity filtered through a 200-μm mesh filter, the filter examined under a stereomicroscope, and swimming zooplankton removed. Three to five replicates per depth were filtered through pre-combusted GF/F filters and used for particulate organic carbon analyses (¼ to ½ of a tube). An additional three samples were filtered through pre-combusted quartz (QMA) filters and used for C:^{234}Th ratio measurements (Stukel et al., 2019). On the P0704, P0810, and P1604 cruises, two replicates (one half tube each) per depth were saved in formaldehyde and analyzed under a stereomicroscope to quantify fecal pellet abundance (Stukel et al., 2013; Morrow et al., 2018). For detailed methods and information on additional analyses made from these traps, see Gutierrez-Rodriguez et al. (2018), Morrow et al. (2018), and Stukel et al. (2019).

^{234}Th Analyses

Water column ^{234}Th activity was measured (typically two profiles per cycle and 10–12 depths per profile, spanning the upper 200 m of the water column) using standard small volume techniques (Benitez-Nelson et al., 2001; Pike et al., 2005). Briefly, 4-L samples were spiked with tracer ^{230}Th and thorium was co-precipitated with manganese oxide. Samples were beta counted on a RISO low-level background beta counter and re-counted >6 half-lives later. Samples were dissolved and spiked with ^{229}Th. The $^{229:230}$Th ratio was determined by inductively coupled plasma mass spectrometry to determine the yield of the initial thorium filtration. For additional details, see Stukel et al. (2019). ^{238}U–^{234}Th deficiency was quantified after determining ^{238}U activity from relationships with salinity published in Owens et al. (2011). ^{238}U–^{234}Th deficiency was combined with sediment trap organic carbon flux measurements to estimate twilight zone CFA as outlined below.

Carbon Flux Attenuation

Within the CCE, which has high mesoscale variability and pronounced horizontal currents, we consider our drifting sediment traps to provide a more accurate estimate of carbon flux than ^{234}Th (see **Supplementary Materials**). Our supposition that the sediment traps have no substantial over- or under-collection bias is supported by a total of 56 paired sediment trap and ^{238}U–^{234}Th deficiency measurements showing good agreement (see "Results" section). Consequently, we use sediment trap values of carbon flux at deployment depths (typically near the base of the euphotic zone and at 100 m) and utilize ^{238}U–^{234}Th measurements to generate smooth profiles of CFA above, between, and below sediment trap deployment depths. Specifically, carbon flux at a depth horizon (D) can be quantified from ^{238}U–^{234}Th deficiency using a steady-state without advection equation:

$$\text{Flux}\,(D) = \text{CTh}(D) \times \int_0^D \lambda_{234} \times \text{Def}(z)dz \quad (1)$$

where CTh(D) is the C:^{234}Th ratio of sinking particles at the depth horizon of interest, λ_{234} is the ^{234}Th decay constant, and Def(z) is the ^{238}U–^{234}Th deficiency at depth z, which is equal to the activity of ^{238}U minus the activity of ^{234}Th. CFA can thus be calculated from the first derivative of Eq. 1:

$$\text{CFA} = \frac{\partial\left(\text{CTh}(D)\right)}{\partial z} \times \int_0^D \left(\lambda_{234} \times \text{Def}(z)\right) dz + \lambda_{234} \times \text{Def}(D) \times \text{CTh}(D) \quad (2)$$

Stukel et al. (2019) found a strong relationship between the C:^{234}Th ratio of sinking particles and the ratio of vertically integrated POC to vertically integrated total water column ^{234}Th (^{V}C:^{234}Th$_{tot}$). Using this equation allows us to determine CTh(D) as a smoothly varying function of D. For additional details see **Supplementary Appendix S1**.

Particle Sinking Speed

We estimate sinking speeds from microscopic analyses of fecal pellets collected in the sediment traps (Stukel et al., 2013; Morrow et al., 2018) and a relationship between fecal pellet size and sinking rate. A strong relationship between size and sinking speed is a consistent finding of studies that have quantified fecal pellet sinking rates (Small et al., 1979; Giesecke et al., 2010; Turner, 2015). Using fecal pellet sinking rate as a function of equivalent spherical diameter (ESD) data reviewed in Stukel et al. (2014), a power-law relationship suggests that sinking speed can be predicted from ESD:

$$\text{SinkingSpeed} = 436 \times \text{ESD}^{0.85} \quad (3)$$

where sinking speed is in units of m day^{-1} and ESD is in units of mm. This relationship is derived from multiple studies spanning a range of taxonomic groups including appendicularians (Ploug et al., 2008), copepods and euphausiids (Smayda, 1971; Turner, 1977; Small et al., 1979; Yoon et al., 2001; Ploug et al., 2008), chaetognaths (Giesecke et al., 2010), and thaliaceans and pteropods (Bruland and Silver, 1981; Madin, 1982; Yoon et al., 2001). We thus expect it to be broadly representative of sinking rates of fecal pellets produced by the mixed zooplankton assemblages encountered in the southern CCE.

Flux-Feeding Calculations

The impact of flux-feeding zooplankters (such as a thecosome pteropod or phaeodarian) on particle flux can be quantified based on the effective cross-sectional area over which particles are collected (Jackson et al., 1993):

$$\frac{\partial F}{\partial z} = -\sigma_x N_x F \quad (4)$$

where F is the flux of sinking particles and N_x is the numerical concentration of suspension feeders (N_{Aulo} is the abundance of Aulosphaeridae and N_{ptero} is the abundance of pteropods; all a function of depth). σ_x is the cross-sectional area over which the organisms are intercepting particles: $\sigma_x = \pi/4 \times \text{ESD}_{eff}^2$. Following Stukel et al. (2018a), ESD$_{eff}$ is the effective diameter over which the organisms collect sinking particles and is dependent on both the diameter of the collection apparatus and

the average cross-sectional area of sinking particles. For the CCE, the effective diameter of sinking fecal pellets was calculated as D_{par} = 403 μm. We then calculate:

$$\sigma_{Aulo} = \frac{\pi}{4}\left(1.25 \times ESD_{Aulo} + D_{par}\right)^2 \quad (5)$$

$$\sigma_{ptero} = \frac{\pi}{4}\left(ESD_{Web} + D_{par}\right)^2 \quad (6)$$

where ESD_{Aulo} is the equivalent spherical diameter of Aulosphaeridae cells (measured separately by UVP5 for each cell) and ESD_{web} is the equivalent spherical diameter of a pteropod feeding web [assumed to be 45 mm based on summary in Gilmer and Harbison (1986)]. The factor of 1.25 in Eq. 6 represents the ratio of cell diameter (reported by UVP5) to diameter including radial spines.

Suspension-Feeding Calculations

The impact of suspension-feeding zooplankton (within which we include both true filter-feeders, e.g., appendicularians, and other organisms such as some herbivorous copepods that may use feeding currents that can be modeled as suspension-feeding) on particle flux attenuation can be calculated as:

$$\frac{\partial F}{\partial z} = -\frac{CR_0}{S} N_x F \quad (7)$$

where N_x is the number concentration of suspension feeders with a clearance rate of CR_0, and S is the sinking speed of the particles. The impact of suspension-feeding zooplankton thus depends on the range of sinking speeds of sinking particles. We calculated clearance rates using the allometric scaling relationship determined in Kiørboe (2011):

$$CR_0 = 10^{a+b\times\log_{10}(BC)} \times Q_{10}^{(T-15)/10} \quad (8)$$

where CR_0 is the clearance rate (mL day^{-1}), BC is the individual carbon content (g), a = 7.31 (±0.27), b = 1.01 (±0.05), and the Q_{10} used to account for temperature effects was assumed (following Hansen et al., 1997) to be 2.8.

We utilized zooplankton data from nighttime MOCNESS tows sorted into broad taxonomic and size groups using ZooScan. The choice to use only nighttime biomass likely leads to a conservative estimate of flux attenuation, because it excludes the activity of diel vertical migrants. This decision was made because these vertical migrants likely feed primarily in the surface layers and are not actively feeding at depth. The carbon biomass of individual organisms was determined using length:carbon relationships for different taxa as outlined in Table 1 of Stukel et al. (2013). We calculated clearance rates for four groups of potentially suspension-feeding mesozooplankton: copepods, euphausiids, appendicularians, and ostracods, while recognizing that some taxa include omnivores or predators. Nauplii and doliolids were also sorted in the samples, but their biomasses were low and hence are not considered further. Other taxa, including chaetognaths, were abundant, but are not suspension feeders.

RESULTS

Carbon Flux and Carbon Flux Attenuation

We used two independent estimates of particle flux (sediment traps and ^{238}U–^{234}Th) to test whether or not our estimates of particle flux (and particle flux attenuation) suffered from methodological biases (**Figure 2**). Comparisons between ^{234}Th flux collected in sediment traps and ^{234}Th flux estimated from ^{238}U:^{234}Th disequilibrium [computed using a one-dimensional, steady-state model without upwelling, Savoye et al. (2006)] showed strong agreement, with occasional outliers. The median ratio of sediment trap-derived flux to deficiency-derived flux was 0.998 suggesting near perfect agreement on a typical deployment. However, the overall mean of the sediment trap dataset was 6% higher than that of the Th deficiency dataset, suggesting that when there was a substantial disagreement, the sediment trap results were likely to be higher. This is not surprising in a dynamic system, where bloom decay can lead to spikes in particle export on faster time-scales than the approximately monthly temporal integration time-scale of ^{238}U–^{234}Th deficiency approaches. The overall agreement between sediment trap and thorium-based approaches suggests that our sediment traps had neither an over- nor an under-collection bias. Furthermore, our results suggest that although ^{234}Th-derived flux may not perfectly match with contemporaneous processes occurring in the surface layer, there is no reason to suspect that flux attenuation calculations based on ^{234}Th measurements will have a systematic bias.

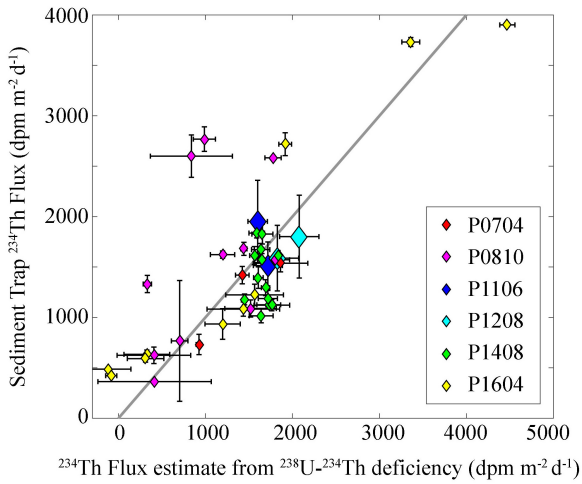

FIGURE 2 | Comparison of sediment trap and ^{238}U–^{234}Th deficiency measurements. *Y*-axis is ^{234}Th flux directly measured in sediment traps. *X*-axis is ^{234}Th flux estimated during the same cycle from ^{238}U–^{234}Th deficiency using a one-dimensional steady-state model without upwelling or diffusion. Note that for the P1106 and P1208 cruises, we plot only two data points each (representing cruise average results at the base of the euphotic zone or at 100 m). These cruise averages were used instead of a separate point for each cycle, because at the smaller spatial scales sampled on these "front" cruises ^{234}Th spatial patterns are likely driven as strongly by advection as by contemporaneous sinking flux.

Across the 30 Lagrangian cycles, POC flux (measured by sediment trap) at 100 m depth ranged from 2.6 to 24.9 mmol C m^{-2} day^{-1}. Export was higher in coastal areas than in the oligotrophic, offshore domain and there was a strong correlation between POC flux and both primary productivity and surface chl. When independent sediment trap export measurements were made at the base of the euphotic zone and at 100 m depth, the correlation (Spearman's ρ) between flux at these two depths was 0.72 (p = 0.002). This across-depth correlation was substantially weaker when only data from frontal regions (P1106 and P1208 Cruises) were analyzed (ρ = 0.49, p = 0.36) than when non-front data were considered (ρ = 0.92, $p = 4.5 \times 10^{-4}$). For all paired samples, the median ratio of sediment trap flux at 100 m to sediment trap flux near the base of the euphotic zone (shallow trap depths varied from 47 to 70 m) was 0.72, suggesting that approximately 28% of sinking POC could be expected to be remineralized before a depth of 100 m on these cycles.

To determine continuous profiles of carbon flux and CFA, we merged sediment trap data with ^{234}Th data. We restricted this flux attenuation analysis to the depth range from the base of the euphotic zone to a depth of 150 m, because at deeper depths we cannot constrain the C:^{234}Th ratio with certainty. The depth range of our flux attenuation calculations thus corresponds with the upper twilight zone, where zooplankton roles in flux attenuation have been hypothesized to be particularly important (Jackson and Checkley, 2011). CFA in the upper twilight zone was highly variable (**Figure 3A**). When comparing across all cycles, flux attenuation decreased with depth from a mean (across all cycles) flux attenuation of 913 μmol C m^{-2} day^{-1} decrease in flux over a 10 m depth range between 80 and 90 m (interquartile range was 57–874 μmol C m^{-2} day^{-1}/10 m) to a mean of 495 μmol C m^{-2} day^{-1}/10 m (interquartile = 328–692 μmol C m^{-2} day^{-1}/10 m) between 140 and 150 m depth. Additional patterns can be seen when considering the oligotrophic and high biomass cycles separately. For the oligotrophic cycles, the base of the euphotic zone (1% light level) was typically in the range of 60–80 m. We thus considered flux attenuation starting at the deeper limit of this range. Flux attenuation increased with depth from a mean of 231 μmol C m^{-2} day^{-1}/10 m (interquartile = −82 to 418.5) in the 80–90 m depth range to a mean of 503 μmol C m^{-2} day^{-1}/10 m (interquartile = 233–799) in the 100–110 m depth range. Beneath this depth flux attenuation declined gradually (**Figure 3B**). For the high biomass cycles a similar pattern was seen. Flux attenuation over the 50–60 m depth range in the high biomass cycles averaged 595 μmol C m^{-2} day^{-1}/10 m (interquartile = −338 to 1221) and increased to 1503 μmol C m^{-2} day^{-1}/10 m (interquartile = 514–1.981) in the 80–90 m depth range.

In contrast to absolute flux attenuation, the percentage of flux remineralized over a 10-m depth range did not decrease beneath 100 m (**Figures 3D–F**). Instead, relative flux attenuation increased somewhat from near the base of the euphotic zone to 150 m. This pattern was relatively consistent when restricting analyses to the oligotrophic cycles (**Figure 3E**), but was less distinct in the high biomass cycles (**Figure 3F**). Nevertheless, across depth and regions, relative CFA was typically in the range of 6–10% of carbon flux remineralized over a 10-m depth range. The median relative flux attenuation in the shallow twilight zone varied from 6.0 to 9.0% of flux/10 m (mean ranged

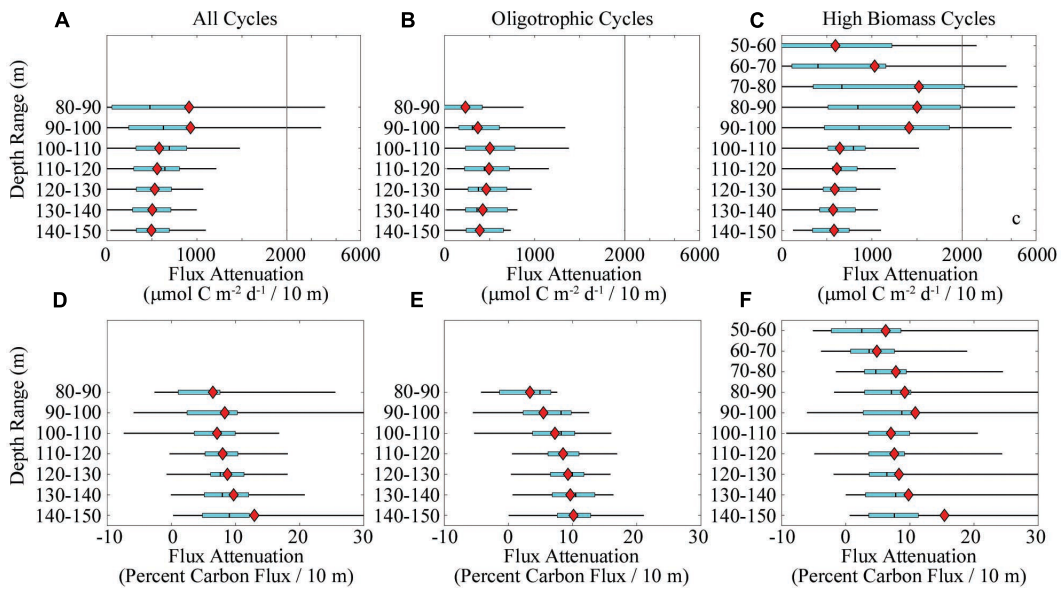

FIGURE 3 | Carbon flux attenuation determined by merging sediment trap and ^{238}U–^{234}Th deficiency data. Panels **(A–C)** show absolute flux attenuation over 10 m depth bins (note break in flux scale at 2000 μmol C m^{-2} day^{-1}/10 m). Panels **(D–F)** show relative flux attenuation over 10 m depth bins. In all panels, light blue boxes show quartiles (median is black line) and thin black lines show 95% confidence intervals (computed using MATLAB function quantile). Red diamonds are arithmetic mean value. Panels **(A)** and **(D)** show data for all cycles. Panels **(B)** and **(E)** show data for cycles with surface chl <0.5 μg Chl a L^{-1}. Panels **(E)** and **(F)** show data for cycles with surface chl >0.5 μg Chl a L^{-1}.

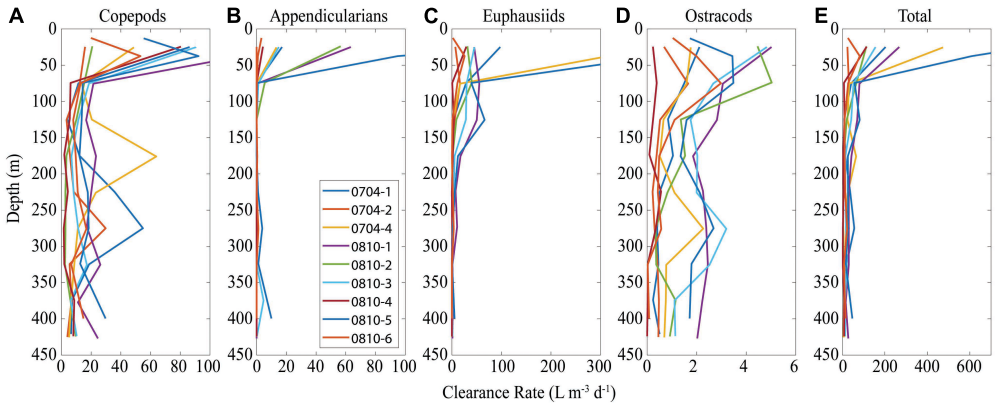

FIGURE 4 | Clearance rates for copepods **(A)**, appendicularians **(B)**, euphausiids **(C)**, ostracods **(D)**, and the sum of all four groups **(E)**. Each plot shows results within 50-m bins as collected by MOCNESS tows and computed using Eq. 8.

from 6.5 to 13%/10 m). This sets a reasonable expectation for the amount of flux attenuation that must be mediated by the combined mesopelagic microbial, mesozooplankton, and nekton communities.

Suspension-Feeding Zooplankton and Particle Flux Attenuation

Suspension-feeding crustaceans are the most abundant (by carbon biomass) ecological category of zooplankton in the CCE (Lavaniegos and Ohman, 2007). To quantify the potential role of these suspension feeders, we utilized data from nighttime MOCNESS tows in the CCE. Suspension-feeder biomass in the mesopelagic was typically dominated by copepods and euphausiids (**Supplementary Figure S2**). Between 100 and 450 m depth, copepod biomass was typically in the range of 1–3 mg C m^{-3}. Euphausiid biomass was almost always <1 mg C m^{-3} at depths deeper than 200 m (and typically <0.4 mg C m^{-3}) but was greater in the shallow mesopelagic. Ostracods had substantially lower biomass, never exceeding 0.6 mg C m^{-3} in the mesopelagic. Appendicularians, while occasionally abundant in the euphotic zone, were also relatively minor contributors to total suspension-feeder biomass in the mesopelagic.

Community clearance rates ranged from 2 to 81 L m^{-3} day^{-1} in the mesopelagic, which corresponds to mesozooplankton clearing between 0.2 and 8.1% of the water each day (**Figure 4**). Clearance rates were dominated by copepods and euphausiids, with copepods dominating beneath 150 m and both having substantial contributions at shallower depths.

The impact of suspension feeders on particle flux attenuation depends on the average sinking rates of particles. We chose P0704-1 as a cycle with typical community clearance rates and calculated flux attenuation for particles with a full range of sinking speeds (**Figure 5**). For particles with a sinking speed of 1 m day^{-1}, nearly all flux would be consumed by suspension feeders within 50 m of the depth of particle creation. By contrast, for particles sinking at a speed of 10 m day^{-1}, only ∼70% of flux would be expected to be consumed before particles reach a depth of 450 m. For particles sinking at a rate of >50 m day^{-1}, the impact of suspension feeders becomes negligible. Comparing data from all cycles, we see a similar pattern. If particles sink at 1 m day^{-1}, anywhere from ∼5 to 50% of sinking particles would be consumed over a 10 m depth range (**Figure 6A**). For particles sinking with a speed of 10 m day^{-1}, particle flux attenuation was typically <4%/10 m and for particles sinking at a speed of 100 m day^{-1}, particle flux attenuation was always <1%/10 m and typically <0.4%/10 m.

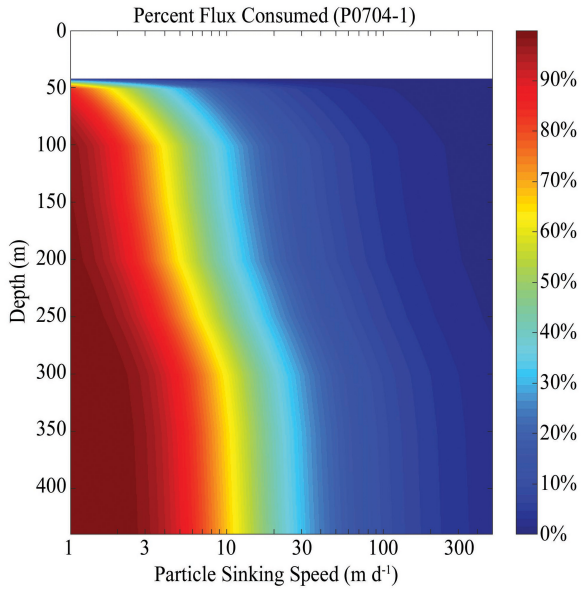

FIGURE 5 | Cumulative percent carbon flux consumed by suspension feeders by a certain depth for particles with different sinking speeds (*x*-axis). Data is for P0704 Cycle 1.

To investigate typical particle sinking speeds, we measured the abundance and size of recognizable fecal pellets collected in sediment traps. These pellets were almost always the dominant visually identifiable component of the sinking material, although

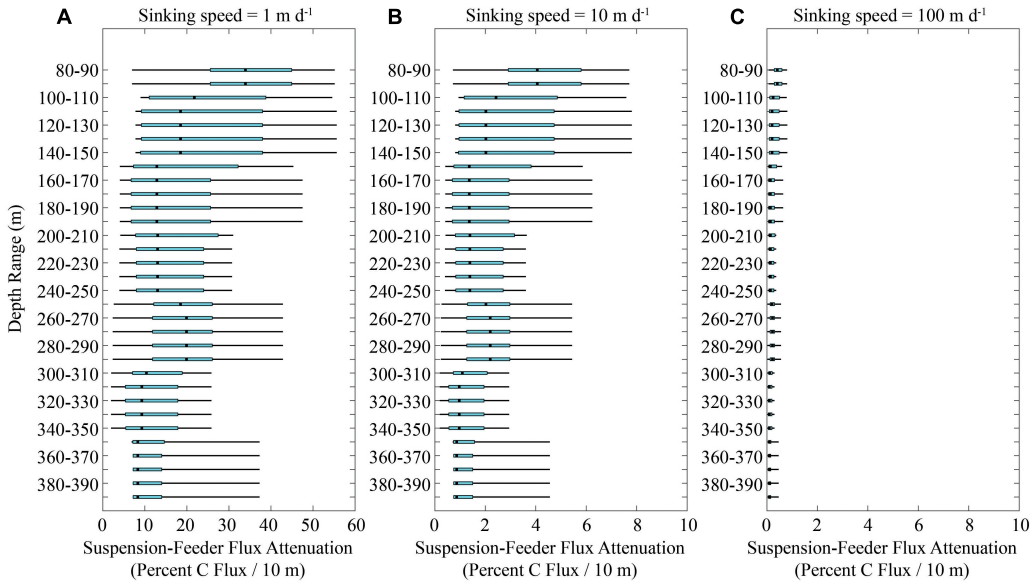

FIGURE 6 | Computed carbon flux attenuation mediated by suspension-feeding copepods, euphausiids, appendicularians, and ostracods if particles are sinking at 1 m day^{-1} **(A)**, 10 m day^{-1} **(B)**, or 100 m day^{-1} **(C)**. Light blue boxes show quartiles (median is black line) and thin black lines show 95% confidence intervals (computed using MATLAB function quantile).

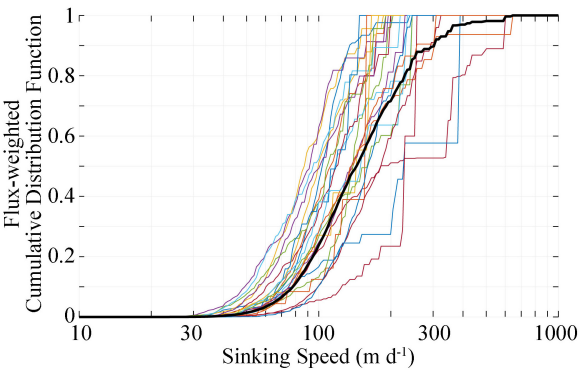

FIGURE 7 | Flux weighted cumulative distribution function for fecal pellets with different sinking speeds. Fecal pellet sinking speeds were calculated from morphometric measurements of fecal pellets collected in sediment traps and Eq. 3. Colored lines are results from individual samples. Black line is the flux-weighted mean of all samples.

in the oligotrophic regions the identifiable pellets typically comprised less than half of total carbon flux. We applied allometric–scaling relationships between sinking speed and fecal pellet size to estimate fecal pellet settling velocities. Across all samples, half of the fecal pellet carbon flux was mediated by pellets sinking at a speed slower than 141 m day^{-1} (**Figure 7**). Only 10% of the flux was due to pellets sinking slower than 78 m day^{-1} and only 1% was derived from pellets sinking slower than 46 m day^{-1}. Even for the cycle most dominated by small fecal pellets, half of the pellet flux was due to pellets sinking faster than 85 m day^{-1}. When considering these results in light of the calculated impact of suspension-feeding zooplankton on flux attenuation of particles with average sinking speeds in the range of 100 m day^{-1}, it becomes clear that suspension-feeding mesozooplankton are not likely to be playing a dominant role in CFA in the mesopelagic. This does not mean, however, that they play no role in flux attenuation. Rather, the abundance and activity of suspension feeders in the epipelagic may be the reason that so few slowly sinking particles were collected in sediment traps beneath the euphotic zone.

Flux-Feeding Zooplankton and Particle Flux Attenuation

To investigate the potential role of flux- feeding zooplankton in CFA, we quantified the abundances of two prominent taxa of flux feeders in the CCE: Aulosphaeridae (a phaeodarian) and *L. helicina* (a thecosome pteropod). These are certainly not the only flux-feeding zooplankton in the CCE, hence our calculations of the total contribution of flux feeders should be considered quite conservative.

Aulosphaeridae abundance consistently peaked in the shallow twilight zone between 50 and 150 m depth (**Figures 8A–E**). Abundances were substantially higher on the P0810 and P1106 cruises (peak cycle average abundances reaching >500 cells m^{-3}) than on the warm period cruises (P1408 and P1604, peak abundances <50 cells m^{-3}). Unlike most other plankton community and biogeochemical measurements, there was not a strong correlation between Aulosphaeridae abundance and primary productivity (cf. Biard and Ohman, 2019). Using Eqs 4 and 5, we quantified the potential impact of Aulosphaeridae on CFA (**Figures 8F–H**). Despite high variability, Aulosphaeridae often had an important role in flux attenuation. Near the depth

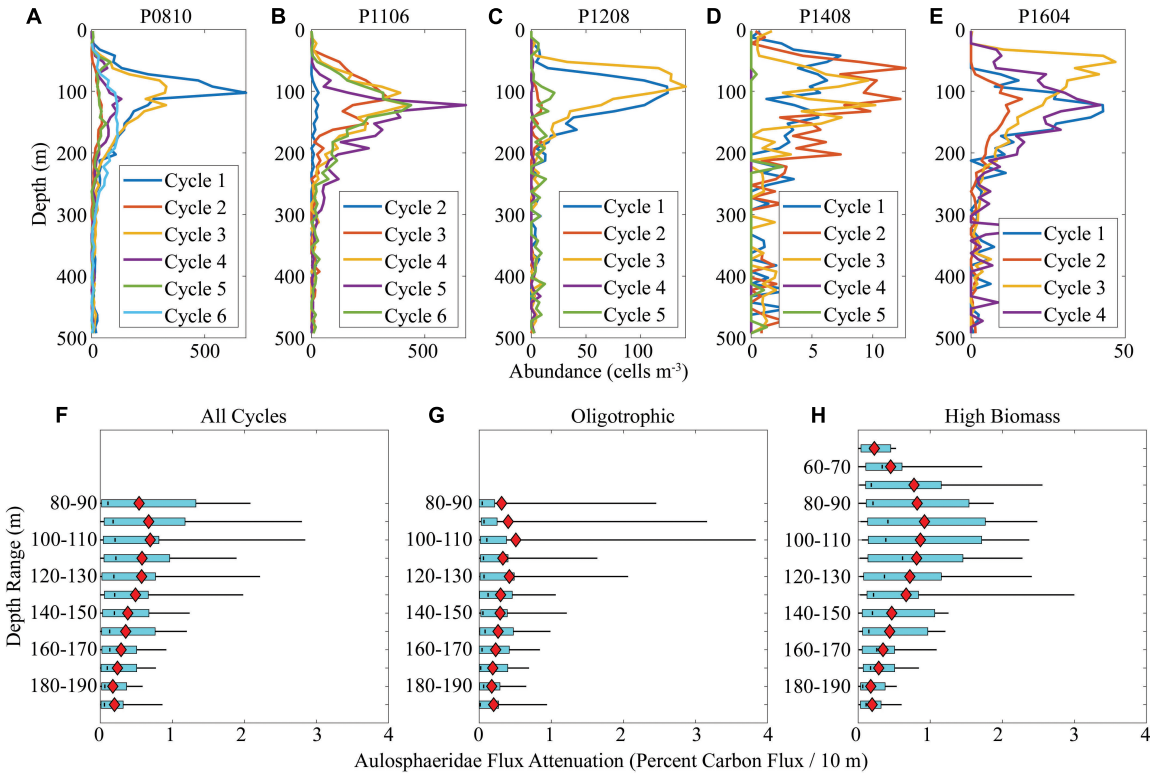

FIGURE 8 | Abundance **(A–E)** and flux attenuation **(F–H)** of Aulosphaeridae. Note the different *x*-axis scales used in panels **(A–E)** that were necessary because of high inter-cruise variability in Aulosphaeridae abundance. Panels **(F–H)** show computed flux attenuation mediated by Aulosphaeridae. Light blue boxes show quartiles (median is black line) and thin black lines show 95% confidence intervals (computed using MATLAB function quantile). Red diamonds are arithmetic mean value.

of peak Aulosphaeridae abundance (∼100 m), the mean (across all cycles) flux attenuation attributable to Aulosphaeridae was 0.69%/10 m (median = 0.21%/10 m, interquartile range = 0.04–0.81%). The maximum Aulosphaeridae flux attenuation (Cycle P0810-1, 100–110 m depth range) was 4.2%/10 m. For comparison, the total flux attenuation mediated by all abiotic and biotic factors (as assessed using sediment traps and ^{234}Th) was typically in the range of 6–10%/10 m. Thus, the Aulosphaeridae (a single family of phaeodarians) can play a substantial role in CFA, although at most times its contribution is <5% of total flux attenuation.

Limacina helicina was only quantified in MOCNESS samples from two cycles (P1208-3, which had a 31-m deep euphotic zone, and P1208-4, which had a 70-m euphotic zone). *L. helicina* abundances typically declined from peak abundances of ∼0.5–2 individuals m^{-3} in the upper 100 m of the water column to <0.2 individuals m^{-3} beneath 100 m depth (**Figure 9A**). We computed (using Eqs 4 and 6) the potential role of *L. helicina* in intercepting sinking particles and found that they could potentially intercept between 4 and 10% of sinking particles between the base of the euphotic zone and a depth of 400 m (**Figure 9B**). However, their impact was concentrated just below the base of the euphotic zone, where on Cycle P1208-3 they consumed an average of 1.2–1.6% of carbon flux/10 m and on P1208-4 they consumed an average of 0.45–0.81%/10 m (**Figures 9C,D**). As for the Aulosphaeridae, the evidence suggests that this species can intercept a substantial portion of the sinking particles, but their impact is concentrated on the region immediately beneath the euphotic zone.

DISCUSSION

Zooplankton as Gatekeepers to the Mesopelagic

Zooplankton play diverse roles in the epi- and mesopelagic (Steinberg and Landry, 2017). Our results show that suspension-feeding mesozooplankton (especially copepods and euphausiids) are abundant in the twilight zone and can have substantial clearance rates on the magnitude of 50 L m^{-3} day^{-1} (**Figure 4** and **Supplementary Figure S2**). However, these clearance rates are not sufficient to give them a meaningful impact on CFA of the particles sinking at ∼100 m day^{-1}, which dominate flux in the region (**Figures 5**, **6**). Instead, their activity leads to near complete consumption of slowly sinking particles near the base of the euphotic zone. This is likely a general result, because studies focused on *in situ* measurement of particle sinking speeds often find typical velocities on the order of 100 m day^{-1} beneath the euphotic zone (Alldredge and Gotschalk, 1988; Trull et al., 2008; Armstrong et al., 2009; McDonnell and Buesseler, 2010;

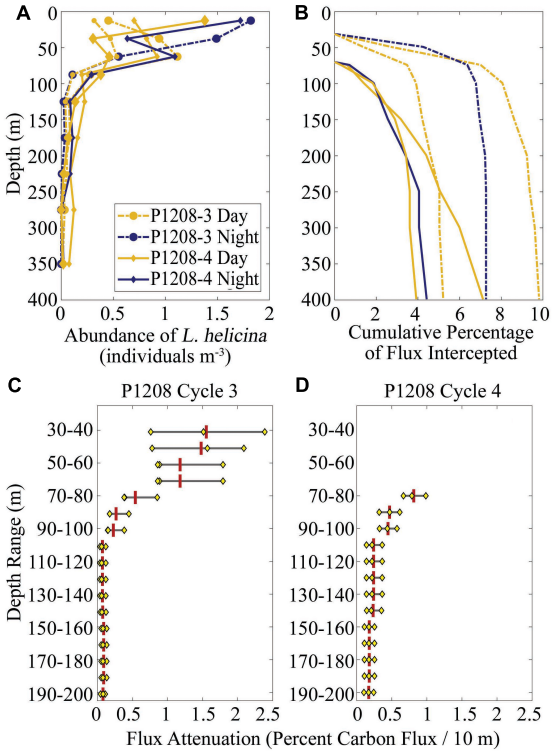

FIGURE 9 | Importance of pteropods to flux attenuation. The abundance of *Limacina helicina* in MOCNESS tows conducted during two cycles on the P1208 cruise from Bednaršek and Ohman (2015) **(A)**. The cumulative percentage of flux intercepted by *L. helicina* based on abundances measured during each MOCNESS tow and assuming a 45-mm diameter for the mucous feeding web **(B)**. Cumulative percentage flux is calculated starting at the base of the euphotic zone (1% light level), which was at 30 m on P1208-3 and 70 m on P1208-4. Panels **(C)** and **(D)** show computed flux attenuation mediated by Aulosphaeridae. Black line shows the range of values measured on the three tows for each Cycle (which are depicted as yellow diamonds). Vertical red line is arithmetic mean.

Jackson et al., 2015). It may also partially explain the rapid decrease in marine snow abundance beneath the euphotic zone (Lampitt et al., 1993; Jackson and Checkley, 2011), particularly if these aggregates are assumed to have heterogeneous compositions that lead to a wide range of sinking speeds.

We also note that our calculations were based on nighttime net tows, thus largely excluding any potential impacts of diel vertically migrating suspension feeders. This decision was based on the assumption that diel vertical migrants feed primarily in the surface layers, not at depth. If we calculate clearance rates based on daytime net tows, we find increased mesopelagic clearance rates, particularly at depths between 150 and 250 m. However, this increased clearance rate (daytime values were typically 50% higher than nighttime values) still resulted in a low impact of suspension-feeders on rapidly sinking (100 m day^{-1}) particles (median across all cycles was <0.4%/10 at all depths), except for Cycle P0810-3. During this cycle, abundant vertically migrating euphausiids were present and, if they were feeding at depth, the total suspension-feeding community could have been responsible for attenuation of 4% of C flux/10 m during daytime hours (in the depth range 200–250 m). Notably, *Euphausia pacifica* (one of the dominant euphausiids in the CCE) has been shown to play an important role in disaggregation of marine snow in the euphotic zone (Dilling and Alldredge, 2000). However, it is unlikely that they swim as rapidly at their daytime resting depths as they do while actively feeding in the surface ocean. It is thus not currently possible to extrapolate their potential impacts on rapidly sinking particles.

Despite their comparatively weak capacity for intercepting rapidly sinking particles, suspension-feeding zooplankton in the mesopelagic have substantial carbon demands in the CCE (Kelly et al., unpublished) and many other ecosystems (Hernández-Leon and Ikeda et al., 2005; Steinberg et al., 2008b; Burd et al., 2010; Robinson et al., 2010; Schukat et al., 2013; Proud et al., 2017). Potential food sources include slowly sinking particles produced in the euphotic zone, free-living mesopelagic protists, particle-attached protists and microbes that may have been released from sinking particles, and carnivory on vertically migrating or mesopelagic resident zooplankton. Slowly sinking particles may also be generated from rapidly sinking particles through the swimming or feeding actions of mesozooplankton (Dilling and Alldredge, 2000; Goldthwait et al., 2004; Iversen and Poulsen, 2007). Indeed, such particle transformations, whether mediated by zooplankton, microbes, or abiotic processes, are likely to continually generate additional slowly sinking particles throughout the water column. However, these slowly sinking particles should not be expected to contribute substantially to particle flux in regions with abundant suspension-feeding zooplankton, because the suspension feeders will efficiently consume slowly sinking particles (e.g., **Figure 6A**).

In contrast, flux-feeding zooplankton can be substantial loss terms for rapidly sinking particles. The mean percentage flux attenuation for Aulosphaeridae in the shallow mesopelagic was 0.69%/10-m depth horizon corresponding to the depth of maximum Aulosphaeridae abundance (**Figure 8**). For comparison, in the same depth range total flux averaged 7.1%/10 m (**Figure 3**). This implies that a single family of giant Rhizaria (∼2-mm) may be responsible for nearly 10% of the flux attenuation in the layer immediately beneath the euphotic zone. Similarly, the pteropod *L. helicina* is abundant beneath the euphotic zone and may be responsible for ∼10–20% of total flux attenuation in the depth ranges where it is most common. These are certainly not the only flux feeders in the CCE. Many other pteropod and rhizarian taxa occur in the CCE (Kling and Boltovskoy, 1995; Bednaršek and Ohman, 2015; Biard and Ohman, 2019). Flux feeding has also been suggested for the copepods *Neocalanus cristatus* and *Spinocalanus antarcticus* (Dagg, 1993; Kosobokova et al., 2002) and the polychaetes *Poeobius* and *Poecilochaetus* (Hamner et al., 1975; Uttal and Buck, 1996; Christiansen et al., 2018). Flux feeding may also be a part-time feeding mode used by a diverse class of organisms during low food periods. For instance, in the absence of phytoplankton prey, the copepod *Acartia tonsa* will behave as a non-motile feeder that will occasionally feed on fecal pellets that pass within its detection radius (Poulsen and Kiorboe, 2005). It is unknown if such behavior is widespread amongst the abundant diel vertically

migrating zooplankton that spend half of their life in the low-prey mesopelagic environment. Another similar strategy has been termed "active flux feeding" or "plume finding" by Stemmann et al. (2004b) and involves cruise-feeding copepods that detect the solute plume behind a sinking aggregate (Kiørboe and Thygesen, 2001), leading to capture rates that are dependent on sinking speed. We could not quantify the impact of this feeding strategy, because the taxa that utilize it have not been identified. However, if it is widespread amongst mesopelagic copepods [as assumed by Stemmann et al. (2004a)] it would lead to substantially greater attenuation of particle flux in the twilight zone.

Also of import, these flux feeders not only intercept and consume sinking particles, but also produce sinking fecal pellets. *L. helicina* fecal pellets have been shown to contribute 19% of the POC flux in a coastal bay near Antarctica (Manno et al., 2009), while "mini-pellets" produced by phaeodarians were abundant contributors to sinking flux in the Eastern Tropical Pacific and Northeast Atlantic (Gowing and Silver, 1985; Lampitt et al., 2009). Furthermore, due to their dense aragonite shells and siliceous tests, respectively, dead pteropods and phaeodarians likely contribute substantially to sinking flux and are often found in sediment trap material (Takahashi and Honjo, 1981; Bathmann et al., 1991; Fabry and Deuser, 1992; Michaels et al., 1995; Biard et al., 2018). Future research will need to focus on the roles of these organisms in transforming not just the quantity but also the quality of sinking particles in the mesopelagic.

Microbes and Zooplankton in the Mesopelagic

The abundance (and impact on flux attenuation) of suspension-feeding and flux-feeding zooplankton generally decreases with depth in the mesopelagic. In particular, the flux-feeding zooplankton that we believe play a disproportionately strong role in twilight zone flux attenuation both decreased sharply in abundance beneath a depth of ∼100 m. However, the percentage (but not absolute magnitude) of CFA increased slightly with depth between 80 and 150 m depth (**Figure 3**). While the substantial variability in flux attenuation profiles prevents us from making definitive conclusions about these patterns, this mismatch between flux attenuation patterns determined from bulk flux estimates (sediment traps and ^{234}Th) and the abundance of flux feeders points to the importance of other sources of carbon remineralization. Stemmann et al. (2004a) suggested based on modeling results for the Mediterranean Sea that flux feeders may be particularly important in the shallow twilight zone, while microbial degradation becomes increasingly important at the lower particle concentrations experienced in deeper waters. Such a result seems plausible for multiple reasons. First, free-living zooplankton will have substantially greater difficulty obtaining sufficient energy for basal metabolic needs and respiration in the deeper ocean, while particle-attached microbes should have ample food at all depths. Second, the abundance of particle-attached microbes on a sinking particle may be expected to increase with age (and depth) of the particle, because it may be continually colonized by new microbes while it sinks, and these microbes are likely to multiply on the sinking particle.

Results from other studies in the CCE can highlight the potential impact of microbes. Simon et al. (1990) estimated that marine snow turnover times with respect to bacterial remineralization ranged from 20 to 100 d. This is similar to the turnover times expected to be mediated by suspension-feeding zooplankton, and suggests that bacteria have only a minor impact on the flux of rapidly sinking particles. However, Samo et al. (2012) measured bacterial carbon production rates (including particle-attached and free-living bacteria) at a depth of 100 m that ranged from ∼10 to 100 μmol C m^{-3} day^{-1}. For comparison, we quantified that the total flux attenuation at this depth was 75 μmol C m^{-3} day^{-1} (median = 66 μmol C m^{-3} day^{-1}; 95% confidence interval of up to 313 μmol C m^{-3} day^{-1}). It is also unclear whether decomposition rates for marine snow aggregates are comparable to those of the fecal pellets that dominate sediment trap material in the CCE. Gowing and Silver (1983) suggested that fecal pellets collected near our study region had substantial contributions of interior bacteria that likely originated as enteric or ingested, but digestion-resistant bacteria. These communities would likely be substantially different, and with different biogeochemical impacts, than those found on aggregates.

Heterotrophic protists can also play dominant roles in the microbial communities consuming fecal pellets (Poulsen and Iversen, 2008). Gutierrez-Rodriguez et al. (2018) used 18S sequencing to investigate protistan sequences in sediment traps on our P1408 cruise. They found a consistent and substantial increase in the relative contribution of dinophytes in un-preserved trap samples relative to formaldehyde-preserved trap samples. Dinophytes typically increased from <10% of total protistan reads to >50%, despite deployment times that were only 3.25 days. Stramenopiles (mainly heterotrophic nanoflagellate taxa) also increased in the unpreserved samples. This suggests potentially rapid growth rates for these protists on sinking particles, with a commensurate role in feeding on either detritus contained in the sinking particles or other microbial taxa transported within the particles.

Multiple studies from other regions have investigated the differing roles of zooplankton and microbes in the mesopelagic (Simon et al., 2002; Robinson et al., 2010; Steinberg and Landry, 2017). Steinberg et al. (2008b) found that bacterial carbon demand exceeded zooplankton demand in the North Pacific subtropical gyre by a factor of 3, although the two were approximately equal in the subarctic gyre. The combined respiration of these two groups was found to be larger than that entering the mesopelagic through sinking particles, a result that has been consistently found in other regions including the subtropical and north Atlantic (Boyd et al., 1999; Reinthaler et al., 2006; Baltar et al., 2009). There are also likely to be extensive synergistic and antagonistic interactions between zooplankton and microbes in the mesopelagic. Zooplankton egestion and excretion at depth provide available organic matter for bacteria (Hannides et al., 2009; Saba et al., 2011; Kiko et al., 2016). Release of organic matter mediated by extracellular enzymes produced by bacteria may contribute to the formation of plumes behind sinking particles that aid zooplankton's abilities to

find such particles (Kiørboe and Thygesen, 2001; Arnosti, 2011). The microbial communities themselves may also serve as nutrient- and carbon-rich food sources for zooplankton (Wilson et al., 2010). It is even possible that fragmentation of particles by mesozooplankton serves to enhance microbial activity and trophic transfer to mesozooplankton (Mayor et al., 2014). Unraveling these potential interactions will require collaborative efforts between microbial and zooplankton ecologists and biogeochemists.

Epipelagic-Mesopelagic Coupling in the CCE

Our result that suspension-feeding zooplankton are abundant in the mesopelagic, but play only minor roles in consuming sinking particles, raises important questions about how they satisfy their metabolic demands. Based on results from our P0704 and P0810 cruises, Kelly et al. (unpublished) estimated that total mesozooplankton (mostly suspension-feeders) respiration in the mesopelagic ranged from 3.2 to 18 mg C m^{-2} day^{-1} across these cruises. These values substantially exceed the total carbon that we calculate suspension-feeders would be able to consume from rapidly sinking particles settling through the mesopelagic. However, the Kelly et al. (unpublished) results also suggest a resolution to this apparent imbalance. Diel vertically migrating taxa were abundant in the region and their active transport provides substantial energy subsidies to mesopelagic food webs. Mesopelagic resident organisms derive energy directly (through predation) and indirectly (through their release of dissolved organic carbon that supports microbial communities) from vertical migrants. Indeed, results showed that nearly half of the organic matter consumed by mesopelagic resident mesozooplankton was derived (directly or indirectly) from foodweb pathways that originated with active transport by vertical migrants rather than pathways originating from sinking particle flux (Kelly et al., unpublished).

This highlights an important reality of mesopelagic ecosystems. Although we most often think of these ecosystems as being supported by sinking particles (and to a lesser extent diel vertical migration), mesopelagic communities feature complex ecological relationships between particle-attached and free-living bacteria, protistan bacterivores, and zooplankton (Robinson et al., 2010). These zooplankton communities are diverse and have many feeding modes including suspension-feeding (likely on protists and suspended organic matter), flux-feeding, predation, and parasitism (Steinberg et al., 2008a; Wilson et al., 2010; Bode et al., 2015). The quality (in addition to quantity) of sinking particles also changes with depth as these particles are modified by microbial and zooplankton communities, new particles are created through defecation, mortality, molting, and discarded feeding webs, and particle size spectra are reshaped by aggregation and disaggregation (Wakeham et al., 1997; Burd and Jackson, 2009; Turner, 2015). Future studies are necessary to fully investigate the impacts of these different feeding traits on the BCP (Barton et al., 2013) and the impacts that future warming, ocean acidification, changes in optical attenuation, and potential shoaling of the oxycline may have on mesopelagic zooplankton communities (Richardson, 2008; Wishner et al., 2013; Cripps et al., 2014; Hauss et al., 2016; Ohman and Romagnan, 2016).

CONCLUSION

Our results offer compelling evidence that two flux-feeding zooplankton taxa (the phaeodarian Aulophaeridae and the pterpopod *L. helicina*) can exert substantial impact on sinking particles in the shallow twilight zone. Both taxa have the capacity to consume greater than 1% of sinking particles per 10-m vertical depth range at the depths at which they are most abundant, which equates to ∼10–20% of total CFA across those same depth ranges (typically the first 50–100 m beneath the euphotic zone). These are unlikely to be the only flux feeders in the mesopelagic. Indeed many other rhizarians and pteropods are found in the CCE and many other taxa are suspected of full or part-time flux-feeding behavior. Flux-feeders are likely particularly important in consuming rapidly sinking particles that would otherwise penetrate into the deep ocean. The abundance of suspension-feeding zooplankton in the ocean suggests that slowly sinking particles will have a relatively minor contribution to sinking carbon flux in the mesopelagic because they will be rapidly consumed. While our results suggest that feeding mode leads to very different biogeochemical importance for these functional groups of zooplankton, substantial work is needed to directly quantify the impact of these organisms *in situ* and to investigate the spatial and temporal distributions of each feeding trait amongst the diverse zooplankton communities found in the ocean (Barton et al., 2013). The qualitatively different impact of each feeding mode on remineralization length scales in the ocean further suggests that flux feeders should be included in modeling efforts undertaken to investigate marine carbon sequestration.

DATA AVAILABILITY

The datasets generated for this study are available on request to the corresponding author.

AUTHOR CONTRIBUTIONS

MS and TK were responsible for the sediment trap and thorium measurements. MO was responsible for the MOCNESS zooplankton data. MO and TB were responsible for the UVP deployments. TB was responsible for the UVP rhizarian analyses. MS wrote the manuscript. All authors edited the final version of the manuscript.

FUNDING

This work was funded by the NSF Bio OCE grants to the CCE LTER Program: OCE-0417616, OCE-1026607, OCE-1637632, and OCE-1614359. A portion of this work was performed at the

National High Magnetic Field Laboratory, which is supported by the National Science Foundation Cooperative Agreement No. DMR-1644779 and the State of Florida.

ACKNOWLEDGMENTS

We thank the captains and crews of the R. V. Melville, R. V. Thompson, and R. V. Sikuliaq as well as our many collaborators in the CCE LTER Program, without them this study would not have been possible. We also thank N. Bednaršek for the pteropod enumerations. Data used in this manuscript can be found on the CCE LTER DataZoo website: https://oceaninformatics.ucsd.edu/datazoo/catalogs/ccelter/datasets.

SUPPLEMENTARY MATERIAL

The Supplementary Material for this article can be found online at: https://www.frontiersin.org/articles/10.3389/fmars.2019.00397/full#supplementary-material

REFERENCES

Alcaraz, M., Almeda, R., Calbet, A., Saiz, E., Duarte, C. M., Lasternas, S., et al. (2010). The role of arctic zooplankton in biogeochemical cycles: respiration and excretion of ammonia and phosphate during summer. *Polar Biol.* 33, 1719–1731. doi: 10.1007/s00300-010-0789-9

Alldredge, A. L. (1976). Discarded appendicularian houses as sources of food, surface habitats, and particulate organic matter in planktonic environments. *Limnol. Oceanogr.* 21, 14–23.

Alldredge, A. L., and Gotschalk, C. (1988). In situ settling behavior of marine snow. *Limnol. Oceanogr.* 33, 339–351. doi: 10.1016/j.scitotenv.2016.09.115

Archibald, K. M., Siegel, D. A., and Doney, S. C. (2019). Modeling the impact of zooplankton diel vertical migration on the carbon export flux of the biological pump. *Global Biogeochem. Cycles* 33, 181–199. doi: 10.1029/2018gb005983

Armstrong, R. A., Peterson, M. L., Lee, C., and Wakeham, S. G. (2009). Settling velocity spectra and the ballast ratio hypothesis. *Deep Sea Res. II* 56, 1470–1478. doi: 10.1016/j.dsr2.2008.11.032

Arnosti, C. (2011). "Microbial extracellular enzymes and the marine carbon cycle," in *Annual Review of Marine Science*, Vol. 3, eds C. A. Carlson and S. J. Giovannoni (Palo Alto: Annual Reviews), 401–425. doi: 10.1146/annurev-marine-120709-142731

Asher, E., Dacey, J., Stukel, M., Long, M., and Tortell, P. (2016). Processes driving seasonal variability in DMS, DMSP, and DMSO concentrations and turnover in coastal Antarctic waters. *Limnol. Oceanogr.* 62, 104–124. doi: 10.1002/lno.10379

Baines, S. B., Chen, X., Twining, B. S., Fisher, N. S., and Landry, M. R. (2016). Factors affecting Fe and Zn contents of mesozooplankton from the Costa Rica Dome. *J. Plankton Res.* 38, 331–347. doi: 10.1093/plankt/fbv098

Baltar, F., Arístegui, J., Gasol, J. M., Sintes, E., and Herndl, G. J. (2009). Evidence of prokaryotic metabolism on suspended particulate organic matter in the dark waters of the subtropical North Atlantic. *Limnol. Oceanogr.* 54, 182–193. doi: 10.4319/lo.2009.54.1.0182

Barton, A. D., Pershing, A. J., Litchman, E., Record, N. R., Edwards, K. F., Finkel, Z. V., et al. (2013). The biogeography of marine plankton traits. *Ecol. Lett.* 16, 522–534. doi: 10.1111/ele.12063

Bathmann, U. V., Noji, T. T., and Von Bodungen, B. (1991). Sedimentation of pteropods in the Norwegian Sea in autumn. *Deep Sea Res. Part A Oceanogr. Res. Pap.* 38, 1341–1360. doi: 10.1016/0198-0149(91)90031-a

Bednaršek, N., Možina, J., Vogt, M., O'brien, C., and Tarling, G. (2012). The global distribution of pteropods and their contribution to carbonate and carbon biomass in the modern ocean. *Earth Syst. Sci. Data* 4, 167–186. doi: 10.5194/essd-4-167-2012

Bednaršek, N., and Ohman, M. D. (2015). Changes in pteropod distributions and shell dissolution across a frontal system in the California current system. *Mar. Ecol. Progr. Ser.* 523, 93–103. doi: 10.3354/meps11199

Benitez-Nelson, C. R., Buesseler, K. O., Van Der Loeff, M. R., Andrews, J., Ball, L., Crossin, G., et al. (2001). Testing a new small-volume technique for determining Th-234 in seawater. *J. Radioanal. Nuclear Chem.* 248, 795–799.

Bianchi, D., Galbraith, E. D., Carozza, D. A., Mislan, K. A. S., and Stock, C. A. (2013). Intensification of open-ocean oxygen depletion by vertically migrating animals. *Nat. Geosci.* 6, 545–548. doi: 10.1038/ngeo1837

Biard, T., Krause, J. W., Stukel, M. R., and Ohman, M. D. (2018). The significance of giant phaeodarians (Rhizaria) to biogenic silica export in the california current ecosystem. *Global Biogeochem. Cycles* 32, 987–1004. doi: 10.1029/2018gb005877

Biard, T., and Ohman, M. D. (2019). Vertical niche definition of test-bearing protists (Rhizaria) into the twilight zone revealed by in situ imaging. *bioRxiv*

Biard, T., Stemmann, L., Picheral, M., Mayot, N., Vandromme, P., Hauss, H., et al. (2016). In situ imaging reveals the biomass of giant protists in the global ocean. *Nature* 532, 504–507. doi: 10.1038/nature17652

Bode, M., Hagen, W., Schukat, A., Teuber, L., Fonseca-Batista, D., Dehairs, F., et al. (2015). Feeding strategies of tropical and subtropical calanoid copepods throughout the eastern Atlantic Ocean - Latitudinal and bathymetric aspects. *Progr. Oceanogr.* 138, 268–282. doi: 10.1016/j.pocean.2015.10.002

Boyd, P. W., Sherry, N. D., Berges, J. A., Bishop, J. K. B., Calvert, S. E., Charette, M. A., et al. (1999). Transformations of biogenic particulates from the pelagic to the deep ocean realm. *Deep Sea Res. Part II Top. Stud. Oceanogr.* 46, 2761–2792. doi: 10.1016/s0967-0645(99)00083-1

Bruland, K. W., and Silver, M. W. (1981). Sinking rates of fecal pellets from gelatinous zooplankton (salps, pteropods, doliolids). *Mar. Biol.* 63, 295–300. doi: 10.1007/bf00395999

Buitenhuis, E., Le Quere, C., Aumont, O., Beaugrand, G., Bunker, A., Hirst, A., et al. (2006). Biogeochemical fluxes through mesozooplankton. *Global Biogeochem. Cycles* 20:18.

Burd, A. B., Hansell, D. A., Steinberg, D. K., Anderson, T. R., Aristegui, J., Baltar, F., et al. (2010). Assessing the apparent imbalance between geochemical and biochemical indicators of meso- and bathypelagic biological activity: what the @$#! is wrong with present calculations of carbon budgets? *Deep Sea Res. II* 57, 1557–1571. doi: 10.1016/j.dsr2.2010.02.022

Burd, A. B., and Jackson, G. A. (2009). Particle Aggregation. *Annu. Rev. Mar. Sci.* 1, 65–90.

Christiansen, S., Hoving, H.-J., Schütte, F., Hauss, H., Karstensen, J., Körtzinger, A., et al. (2018). Particulate matter flux interception in oceanic mesoscale eddies by the polychaete Poeobius sp. *Limnol. Oceanogr.* 63, 2093–2109. doi: 10.1002/lno.10926

Cripps, G., Lindeque, P., and Flynn, K. J. (2014). Have we been underestimating the effects of ocean acidification in zooplankton? *Glob. Chang. Biol.* 20, 3377–3385. doi: 10.1111/gcb.12582

Dagg, M. (1993). Sinking particles as a possible source of nutrition for the large calanoid copepod Neocalanus cristatus in the subarctic Pacific Ocean. *Deep Sea Res. Part I* 40, 1431–1445. doi: 10.1016/0967-0637(93)90121-i

DeVries, T., Primeau, F., and Deutsch, C. (2012). The sequestration efficiency of the biological pump. *Geophys. Res. Lett.* 39:L13601. doi: 10.1029/2012GL051963

DeVries, T., and Weber, T. (2017). The export and fate of organic matter in the ocean: new constraints from combining satellite and oceanographic tracer observations. *Global Biogeochem. Cycles* 31, 535–555. doi: 10.1002/2016gb005551

Dilling, L., and Alldredge, A. L. (2000). Fragmentation of marine snow by swimming macrozooplankton: a new process impacting carbon cycling in the sea. *Deep Sea Res. I* 47, 1227–1245. doi: 10.1016/s0967-0637(99)00105-3

Ducklow, H. W., Steinberg, D. K., and Buesseler, K. O. (2001). Upper ocean carbon export and the biological pump. *Oceanography* 14, 50–58. doi: 10.5670/oceanog.2001.06

Fabry, V., and Deuser, W. (1992). Seasonal changes in the isotopic compositions and sinking fluxes of euthecosomatous pteropod shells in the Sargasso Sea. *Paleoceanography* 7, 195–213. doi: 10.1029/91pa03138

Fowler, S. W. (1977). Trace elements in zooplankton particulate products. *Nature* 269:51. doi: 10.1038/269051a0

Frangoulis, C., Christou, E. D., and Hecq, J. H. (2005). "Comparison of marine copepod outfluxes: nature, rate, fate and role in the carbon and nitrogen cycles," in *Advances in Marine Biology*, Vol. 47, ed. D. Smith (London: Academic Press Ltd.), 253–309. doi: 10.1016/s0065-2881(04)47004-7

Fuchs, H. L., and Franks, P. J. S. (2010). Plankton community properties determined by nutrients and size-selective feeding. *Mar. Ecol. Progr. Ser.* 413, 1–15. doi: 10.3354/meps08716

Giesecke, R., Gonzalez, H. E., and Bathmann, U. (2010). The role of the chaetognath Sagitta gazellae in the vertical carbon flux of the Southern Ocean. *Polar Biol.* 33, 293–304. doi: 10.1007/s00300-009-0704-4

Gilmer, R., and Harbison, G. (1986). Morphology and field behavior of pteropod molluscs: feeding methods in the families Cavoliniidae, Limacinidae and Peraclididae (Gastropoda: Thecosomata). *Mar. Biol.* 91, 47–57. doi: 10.1007/bf00397570

Glibert, P. M. (1998). Interactions of top-down and bottom-up control in planktonic nitrogen cycling. *Hydrobiologia* 363, 1–12. doi: 10.1073/pnas.0809671106

Goericke, R. (2002). Top-down control of phytoplankton biomass and community structure in the monsoonal Arabian Sea. *Limnol. Oceanogr.* 47, 1307–1323. doi: 10.4319/lo.2002.47.5.1307

Goldthwait, S., Yen, J., Brown, J., and Alldredge, A. (2004). Quantification of marine snow fragmentation by swimming euphausiids. *Limnol. Oceanogr.* 49, 940–952. doi: 10.4319/lo.2004.49.4.0940

Gorokhova, E., Soerensen, A. L., and Motwani, N. H. (2018). Mercury-methylating bacteria are associated with zooplankton: a proof-of-principle survey in the Baltic Sea. *bioRxiv*

Gorsky, G., Ohman, M. D., Picheral, M., Gasparini, S., Stemmann, L., Romagnan, J. B., et al. (2010). Digital zooplankton image analysis using the ZooScan integrated system. *J. Plankton Res.* 32, 285–303. doi: 10.1093/plankt/fbp124

Gowing, M. (1989). Abundance and feeding ecology of Antarctic phaeodarian radiolarians. *Mar. Biol.* 103, 107–118. doi: 10.1007/bf00391069

Gowing, M. M. (1986). Trophic biology of phaeodarian radiolarians and flux of living radiolarians in the upper 2000 m of the North Pacific central gyre. *Deep Sea Res.* 33, 655–674. doi: 10.1016/0198-0149(86)90059-2

Gowing, M. M., and Bentham, W. N. (1994). Feeding ecology of phaeodarian radiolarians at the VERTEX North Pacific time series site. *J. Plankton Res.* 16, 707–719. doi: 10.1093/plankt/16.6.707

Gowing, M. M., and Silver, M. W. (1983). Origins and microenvironments of bacteria mediating fecal pellet decomposition in the sea. *Mar. Biol.* 73, 7–16. doi: 10.1007/bf00396280

Gowing, M. M., and Silver, M. W. (1985). Minipellets - a new and abundant size class of marine fecal pellets. *J. Mar. Res.* 43, 395–418. doi: 10.1357/002224085788438676

Gutierrez-Rodriguez, A., Stukel, M. R., Lopes Dos Santos, A., Biard, T., Scharek, R., Vaulot, D., et al. (2018). High contribution of Rhizaria (Radiolaria) to vertical export in the California Current Ecosystem revealed by DNA metabarcoding. *ISME J.* 13, 964–976. doi: 10.1038/s41396-018-0322-7

Hamner, W., Madin, L., Alldredge, A., Gilmer, R., and Hamner, P. (1975). Underwater observations of gelatinous zooplankton: Sampling problems, feeding biology, and behavior1. *Limnol. Oceanogr.* 20, 907–917. doi: 10.4319/lo.1975.20.6.0907

Hannides, C. C. S., Landry, M. R., Benitez-Nelson, C. R., Styles, R. M., Montoya, J. P., and Karl, D. M. (2009). Export stoichiometry and migrant-mediated flux of phosphorus in the North Pacific Subtropical Gyre. *Deep Sea Res. I* 56, 73–88. doi: 10.1016/j.dsr.2008.08.003

Hansen, J. L. S., Kiorboe, T., and Alldredge, A. L. (1996). Marine snow derived from abandoned larvacean houses: sinking rates, particle content and mechanisms of aggregate formation. *Mar. Ecol. Progr. Ser.* 141, 205–215. doi: 10.3354/meps141205

Hansen, P. J., Bjornsen, P. K., and Hansen, B. W. (1997). Zooplankton grazing and growth: scaling within the 2-2,000-mu m body size range. *Limnol. Oceanogr.* 42, 687–704. doi: 10.4319/lo.1997.42.4.0687

Hauss, H., Christiansen, S., Schütte, F., Kiko, R., Edvam Lima, M., Rodrigues, E., et al. (2016). Dead zone or oasis in the open ocean? Zooplankton distribution and migration in low-oxygen modewater eddies. *Biogeosciences* 13, 1977–1989. doi: 10.5194/bg-13-1977-2016

Henson, S. A., Sanders, R., Madsen, E., Morris, P. J., Le Moigne, F., and Quartly, G. D. (2011). A reduced estimate of the strength of the ocean's biological carbon pump. *Geophys. Res. Lett.* 38:L04606.

Hernandez-Leon, S., and Ikeda, T. (2005). A global assessment of mesozooplankton respiration in the ocean. *J. Plankton Res.* 27, 153–158. doi: 10.3389/fmicb.2017.01358 doi: 10.1093/plankt/fbh166

Hunt, B., Strugnell, J., Bednarsek, N., Linse, K., Nelson, R. J., Pakhomov, E., et al. (2010). Poles apart: the "bipolar" pteropod species *Limacina helicina* is genetically distinct between the Arctic and Antarctic oceans. *PLoS One* 5:e9835. doi: 10.1371/journal.pone.0009835

Iversen, M. H., and Poulsen, L. K. (2007). Coprorhexy, coprophagy, and coprochaly in the copepods *Calanus helgolandicus*, *Pseudocalanus elongatus*, and *Oithona similis*. *Mar. Ecol. Progr. Ser.* 350, 79–89. doi: 10.1021/acs.est.5b05905

Jackson, G. A., Checkley, D. M. Jr., and Dagg, M. (2015). Settling of particles in the upper 100 m of the ocean detected with autonomous profiling floats off California. *Deep Sea Res. I* 99, 75–86. doi: 10.1016/j.dsr.2015.02.001

Jackson, G. A., and Checkley, D. M. (2011). Particle size distributions in the upper 100 m water column and their implications for animal feeding in the plankton. *Deep Sea Res. I* 58, 283–297. doi: 10.1016/j.dsr.2010.12.008

Jackson, G. A., Najjar, R. G., and Toggweiler, J. R. (1993). Flux feeding as a mechanism for zooplankton grazing and its implications for vertical particulate flux. *Limnol. Oceanogr.* 38, 1328–1331. doi: 10.4319/lo.1993.38.6.1328

Kiko, R., Hauss, H., Buchholz, F., and Melzner, F. (2016). Ammonium excretion and oxygen respiration of tropical copepods and euphausiids exposed to oxygen minimum zone conditions. *Biogeosciences* 13, 2241–2255. doi: 10.5194/bg-13-2241-2016

Kiørboe, T. (2011). How zooplankton feed: mechanisms, traits and trade-offs. *Biol. Rev.* 86, 311–339. doi: 10.1111/j.1469-185x.2010.00148.x

Kiørboe, T., and Thygesen, U. H. (2001). Fluid motion and solute distribution around sinking aggregates. II. Implications for remote detection by colonizing zooplankters. *Mar. Ecol. Progr. Ser.* 211, 15–25. doi: 10.3354/meps211015

Kling, S. A., and Boltovskoy, D. (1995). Radiolarian vertical distribution patterns across the southern California current. *Deep Sea Res. I* 42, 191–231. doi: 10.1016/0967-0637(94)00038-t

Knauer, G. A., Martin, J. H., and Bruland, K. W. (1979). Fluxes of particulate carbon, nitrogen, and phosphorus in the upper water column of the Northeast Pacific. *Deep Sea Res.* 26, 97–108. doi: 10.1016/0198-0149(79)90089-x

Komar, P. D., Morse, A. P., Small, L. F., and Fowler, S. W. (1981). An analysis of sinking rates of natural copepod and euphausiid fecal pellets. *Limnol. Oceanogr.* 26, 172–180. doi: 10.4319/lo.1981.26.1.0172

Kosobokova, K., Hirche, H.-J., and Scherzinger, T. (2002). Feeding ecology of Spinocalanus antarcticus, a mesopelagic copepod with a looped gut. *Mar. Biol.* 141, 503–511. doi: 10.1007/s00227-002-0848-z

Lalli, C. M., and Gilmer, R. W. (1989). *Pelagic Snails: The Biology of Holoplanktonic Gastropod Mollusks*. Palo Alto, CA: Stanford University Press.

Lampitt, R., Salter, I., and Johns, D. (2009). Radiolaria: major exporters of organic carbon to the deep ocean. *Global Biogeochem. Cycles* 23:GB1010.

Lampitt, R., Wishner, K., Turley, C., and Angel, M. (1993). Marine snow studies in the Northeast Atlantic Ocean: distribution, composition and role as a food source for migrating plankton. *Mar. Biol.* 116, 689–702. doi: 10.1007/bf00355486

Landry, M. R., Ohman, M. D., Goericke, R., Stukel, M. R., Barbeau, K. A., Bundy, R., et al. (2012). Pelagic community responses to a deep-water front in the California current ecosystem: overview of the A-front study. *J. Plankton Res.* 34, 739–748. doi: 10.1093/plankt/fbs025

Landry, M. R., Ohman, M. D., Goericke, R., Stukel, M. R., and Tsyrklevich, K. (2009). Lagrangian studies of phytoplankton growth and grazing relationships in a coastal upwelling ecosystem off Southern California. *Prog. Oceanogr.* 83, 208–216. doi: 10.1016/j.pocean.2009.07.026

Lavaniegos, B. E., and Ohman, M. D. (2007). Coherence of long-term variations of zooplankton in two sectors of the California current system. *Prog. Oceanogr.* 75, 42–69. doi: 10.1016/j.pocean.2007.07.002

Laws, E. A., D'sa, E., and Naik, P. (2011). Simple equations to estimate ratios of new or export production to total production from satellite-derived estimates of sea surface temperature and primary production. *Limnol. Oceanogr. Methods* 9, 593–601. doi: 10.4319/lom.2011.9.593

Lomas, M., Steinberg, D. K., Dickey, T., Carlson, C., Nelson, N., Condon, R. H., et al. (2010). Increased ocean carbon export in the sargasso sea linked to climate variability is countered by its enhanced mesopelagic attenuation. *Biogeosciences* 7, 57–70. doi: 10.5194/bg-7-57-2010

Madin, L. P. (1982). Production, composition, and sedimentation of salp fecal pellets in oceanic waters. *Mar. Biol.* 67, 39–45. doi: 10.1007/bf00397092

Manno, C., Tirelli, V., Accornero, A., and Fonda Umani, S. (2009). Importance of the contribution of *Limacina helicina* faecal pellets to the carbon pump in Terra Nova Bay (Antarctica). *J. Plankton Res.* 32, 145–152. doi: 10.1093/plankt/fbp108

Mayor, D. J., Sanders, R., Giering, S. L., and Anderson, T. R. (2014). Microbial gardening in the ocean's twilight zone: detritivorous metazoans benefit from fragmenting, rather than ingesting, sinking detritus: fragmentation of refractory detritus by zooplankton beneath the euphotic zone stimulates the harvestable production of labile and nutritious microbial biomass. *Bioessays* 36, 1132–1137. doi: 10.1002/bies.201400100

McDonnell, A. M. P., and Buesseler, K. O. (2010). Variability in the average sinking velocity of marine particles. *Limnol. Oceanogr.* 55, 2085–2096. doi: 10.4319/lo.2010.55.5.2085

Michaels, A. F., Caron, D. A., Swanberg, N. R., Howse, F. A., and Michaels, C. M. (1995). Planktonic sarcodines (Acantharia, Radiolaria, Foraminifera) in surface waters near Bermuda: abundance, biomass and vertical flux. *J. Plankton Res.* 17, 131–163. doi: 10.1093/plankt/17.1.131

Morrow, R. M., Ohman, M. D., Goericke, R., Kelly, T. B., Stephens, B. M., and Stukel, M. R. (2018). Primary productivity, mesozooplankton grazing, and the biological pump in the california current ecosystem: variability and response to El niño. *Deep Sea Res. I* 140, 52–62. doi: 10.1016/j.dsr.2018.07.012

Nakamura, Y., and Suzuki, N. (2015). "Phaeodaria: diverse marine cercozoans of world-wide distribution," in *Marine Protists*, eds S. Ohtsuka, T. Suzaki, T. Horiguchi, N. Suzuki, and F. Not (Berlin: Springer), 223–249. doi: 10.1007/978-4-431-55130-0_9

Ohman, M. D., Powell, J. R., Picheral, M., and Jensen, D. W. (2012). Mesozooplankton and particulate matter responses to a deep-water frontal system in the southern California current system. *J. Plankton Res.* 34, 815–827. doi: 10.1093/plankt/fbs028

Ohman, M. D., and Romagnan, J. B. (2016). Nonlinear effects of body size and optical attenuation on diel vertical migration by zooplankton. *Limnol. Oceanogr.* 61, 765–770. doi: 10.1002/lno.10251

Owens, S. A., Buesseler, K. O., and Sims, K. W. W. (2011). Re-evaluating the 238U-salinity relationship in seawater: implications for the 238U-234Th disequilibrium method. *Mar. Chem.* 127, 31–39. doi: 10.1016/j.marchem.2011.07.005

Picheral, M., Guidi, L., Stemmann, L., Karl, D. M., Iddaoud, G., and Gorsky, G. (2010). The underwater vision profiler 5: an advanced instrument for high spatial resolution studies of particle size spectra and zooplankton. *Limnol. Oceanogr. Methods* 8, 462–473. doi: 10.4319/lom.2010.8.462

Pike, S. M., Buesseler, K. O., Andrews, J., and Savoye, N. (2005). Quantification of 234Th recovery in small volume sea water samples by inductively coupled plasma-mass spectrometry. *J. Radioanal. Nucl. Chem.* 263, 355–360. doi: 10.1007/s10967-005-0594-z

Ploug, H., Iversen, M. H., and Fischer, G. (2008). Ballast, sinking velocity, and apparent diffusivity within marine snow and zooplankton fecal pellets: implications for substrate turnover by attached bacteria. *Limnol. Oceanogr.* 53, 1878–1886. doi: 10.4319/lo.2008.53.5.1878

Poulsen, L. K., and Iversen, M. H. (2008). Degradation of copepod fecal pellets: key role of protozooplankton. *Mar. Ecol. Prog. Ser.* 367, 1–13. doi: 10.3354/meps07611

Poulsen, L. K., and Kiorboe, T. (2005). Coprophagy and coprorhexy in the copepods *Acartia tonsa* and *Temora longicornis*: clearance rates and feeding behaviour. *Mar. Ecol. Prog. Ser.* 299, 217–227. doi: 10.3354/meps299217

Powell, J. R., and Ohman, M. D. (2015). Changes in zooplankton habitat, behavior, and acoustic scattering characteristics across glider-resolved fronts in the Southern California current system. *Prog. Oceanogr.* 134, 77–92. doi: 10.1016/j.pocean.2014.12.011

Proud, R., Cox, M. J., and Brierley, A. S. (2017). Biogeography of the global ocean's mesopelagic zone. *Curr. Biol.* 27, 113–119. doi: 10.1016/j.cub.2016.11.003

Reinthaler, T., Van Aken, H., Veth, C., Arístegui, J., Robinson, C., Williams, P. J. L. B., et al. (2006). Prokaryotic respiration and production in the meso-and bathypelagic realm of the eastern and western North Atlantic basin. *Limnol. Oceanogr.* 51, 1262–1273. doi: 10.4319/lo.2006.51.3.1262

Richardson, A. J. (2008). In hot water: zooplankton and climate change. *Ices J. Mar. Sci.* 65, 279–295. doi: 10.1093/icesjms/fsn028

Robinson, C., Steinberg, D. K., Anderson, T. R., Arístegui, J., Carlson, C. A., Frost, J. R., et al. (2010). Mesopelagic zone ecology and biogeochemistry – a synthesis. *Deep Sea Res. II* 57, 1504–1518. doi: 10.1016/j.dsr2.2010.02.018

Robison, B. H., Reisenbichler, K. R., and Sherlock, R. E. (2005). Giant larvacean houses: rapid carbon transport to the deep sea floor. *Science* 308, 1609–1611. doi: 10.1126/science.1109104

Saba, G. K., Steinberg, D. K., and Bronk, D. A. (2011). The relative importance of sloppy feeding, excretion, and fecal pellet leaching in the release of dissolved carbon and nitrogen by Acartia tonsa copepods. *J. Exp. Mar. Biol. Ecol.* 404, 47–56. doi: 10.1016/j.jembe.2011.04.013

Samo, T. J., Pedler, B. E., Ball, G. I., Pasulka, A. L., Taylor, A. G., Aluwihare, L. I., et al. (2012). Microbial distribution and activity across a water mass frontal zone in the California current ecosystem. *J. Plankton Res.* 34, 802–814. doi: 10.1093/plankt/fbs048

Savoye, N., Benitez-Nelson, C., Burd, A. B., Cochran, J. K., Charette, M., Buesseler, K. O., et al. (2006). 234Th sorption and export models in the water column: a review. *Mar. Chem.* 100, 234–249. doi: 10.1016/j.marchem.2005.10.014

Schmidt, K., Schlosser, C., Atkinson, A., Fielding, S., Venables, H. J., Waluda, C. M., et al. (2016). Zooplankton gut passage mobilizes lithogenic iron for ocean productivity. *Curr. Biol.* 26, 2667–2673. doi: 10.1016/j.cub.2016.07.058

Schukat, A., Bode, M., Auel, H., Carballo, R., Martin, B., Koppelmann, R., et al. (2013). Pelagic decapods in the northern benguela upwelling system: distribution, ecophysiology and contribution to active carbon flux. *Deep Sea Res. Part I Oceanogr. Res. Pap.* 75, 146–156. doi: 10.1016/j.dsr.2013.02.003

Siegel, D. A., Buesseler, K. O., Behrenfeld, M. J., Benitez-Nelson, C. R., Boss, E., Brzezinski, M. A., et al. (2016). Prediction of the export and fate of global ocean net primary production: the EXPORTS science plan. *Front. Mar. Sci.* 3:22. doi: 10.3389/fmars.2016.00022

Siegel, D. A., Buesseler, K. O., Doney, S. C., Sailley, S. F., Behrenfeld, M. J., and Boyd, P. W. (2014). Global assessment of ocean carbon export by combining satellite obervations and food-web models. *Global Biogeochem. Cycles* 28, 181–196. doi: 10.1002/2013gb004743

Silver, M. W., and Gowing, M. M. (1991). The "particle" flux: origins and biological components. *Prog. Oceanogr.* 26, 75–113. doi: 10.1016/0079-6611(91)90007-9

Simon, M., Alldredge, A. L., and Azam, F. (1990). Bacterial carbon dynamics on marine snow. *Mar. Ecol. Prog. Ser.* 65, 205–211. doi: 10.3354/meps065205

Simon, M., Grossart, H. P., Schweitzer, B., and Ploug, H. (2002). Microbial ecology of organic aggregates in aquatic ecosystems. *Aquat. Microb. Ecol.* 28, 175–211. doi: 10.3354/ame028175

Small, L. F., Fowler, S. W., and Unlu, M. Y. (1979). Sinking rates of natural copepod fecal pellets. *Mar. Biol.* 51, 233–241. doi: 10.1021/acs.est.5b05905

Smayda, T. J. (1971). Normal and accelerated sinking of phytoplankton in sea. *Mar. Geol.* 11, 105–122. doi: 10.1016/0025-3227(71)90070-3

Steinberg, D. K., Carlson, C. A., Bates, N. R., Goldthwait, S. A., Madin, L. P., and Michaels, A. F. (2000). Zooplankton vertical migration and the active transport of dissolved organic and inorganic carbon in the Sargasso Sea. *Deep Sea Res. I* 47, 137–158. doi: 10.1016/s0967-0637(99)00052-7

Steinberg, D. K., Cope, J. S., Wilson, S. E., and Kobari, T. (2008a). A comparison of mesopelagic mesozooplankton community structure in the subtropical and subarctic North Pacific Ocean. *Deep Sea Res. II* 55, 1615–1635. doi: 10.1016/j.dsr2.2008.04.025

Steinberg, D. K., Van Mooy, B. A. S., Buesseler, K. O., Boyd, P. W., Kobari, T., and Karl, D. M. (2008b). Bacterial vs. zooplankton control of sinking particle flux in the ocean's twilight zone. *Limnol. Oceanogr.* 53, 1327–1338. doi: 10.1002/bies.201400100

Steinberg, D. K., and Landry, M. R. (2017). Zooplankton and the ocean carbon cycle. *Annu. Rev. Mar. Sci.* 9, 413–444. doi: 10.1146/annurev-marine-010814-015924

Stemmann, L., Jackson, G. A., and Gorsky, G. (2004a). A vertical model of particle size distributions and fluxes in the midwater column that includes biological and physical processes-part II: application to a three year survey in the NW mediterranean sea. *Deep Sea Res. I* 51, 885–908. doi: 10.1016/j.dsr.2004.03.002

Stemmann, L., Jackson, G. A., and Ianson, D. (2004b). A vertical model of particle size distributions and fluxes in the midwater column that includes biological and physical processes-part I: model formulation. *Deep Sea Res. I* 51, 865–884. doi: 10.1016/j.dsr.2004.03.001

Stukel, M. R., Kahru, M., Benitez-Nelson, C. R., Decima, M., Goericke, R., Landry, M. R., et al. (2015). Using lagrangian-based process studies to test satellite algorithms of vertical carbon flux in the eastern North Pacific Ocean. *J. Geophys. Res. Oceans* 120, 7208–7222. doi: 10.1002/2015jc011264

Stukel, M. R., Biard, T., Krause, J., and Ohman, M. D. (2018a). Large phaeodaria in the twilight zone: their role in the carbon cycle. *Limnol. Oceanogr.* 63, 2579–2594. doi: 10.1002/lno.10961

Stukel, M. R., Décima, M., Landry, M. R., and Selph, K. E. (2018b). Nitrogen and isotope flows through the costa rica dome upwelling ecosystem: the crucial mesozooplankton role in export flux. *Global Biogeochem. Cycles* 32, 1815–1832. doi: 10.1029/2018gb005968

Stukel, M. R., Kelly, T. B., Aluwihare, L. I., Barbeau, K. A., Goericke, R., Krause, J. W., et al. (2019). The carbon:234thorium ratios of sinking particles in the California current ecosystem 1: relationships with plankton ecosystem dynamics. *Mar. Chem.* 212, 1–15. doi: 10.1016/j.marchem.2019.01.003

Stukel, M. R., Mislan, K. A. S., Décima, M., and Hmelo, L. (2014). "Detritus in the pelagic ocean," in *Eco-DAS IX Symposium Proceedings*, ed. P. F. Kemp (Waco, TX: Association for the Sciences of Limnology and Oceanography), 49–76.

Stukel, M. R., Ohman, M. D., Benitez-Nelson, C. R., and Landry, M. R. (2013). Contributions of mesozooplankton to vertical carbon export in a coastal upwelling system. *Mar. Ecol. Prog. Ser.* 491, 47–65. doi: 10.3354/meps10453

Takahashi, K., and Honjo, S. (1981). vertical flux of radiolaria: a taxon-quantitative sediment trap study from the Western Tropical Atlantic. *Micropaleontology* 27, 140–190.

Trull, T. W., Bray, S. G., Buesseler, K. O., Lamborg, C. H., Manganini, S., Moy, C., et al. (2008). In situ measurement of mesopelagic particle sinking rates and the control of carbon transfer to the ocean interior during the vertical flux in the global ocean (VERTIGO) voyages in the North Pacific. *Deep Sea Res. II* 55, 1684–1695. doi: 10.1016/j.dsr2.2008.04.021

Turner, J. T. (1977). Sinking rates of fecal pellets from marine copepod *Pontella meadii*. *Mar. Biol.* 40, 249–259. doi: 10.1007/bf00390880

Turner, J. T. (2002). Zooplankton fecal pellets, marine snow and sinking phytoplankton blooms. *Aquat. Microb. Ecol.* 27, 57–102. doi: 10.3354/ame027057

Turner, J. T. (2015). Zooplankton fecal pellets, marine snow, phytodetritus and the ocean's biological pump. *Prog. Oceanogr.* 130, 205–248. doi: 10.1016/j.pocean.2014.08.005

Uttal, L., and Buck, K. (1996). Dietary study of the midwater polychaete poeobius meseres in monterey bay, California. *Mar. Biol.* 125, 333–343. doi: 10.1007/bf00346314

Wakeham, S. G., Lee, C., Hedges, J. I., Hernes, P. J., and Peterson, M. J. (1997). Molecular indicators of diagenetic status in marine organic matter. *Geochim. Cosmochim. Acta* 61, 5363–5369. doi: 10.1016/s0016-7037(97)00312-8

Wilson, S. E., Steinberg, D. K., and Buesseler, K. O. (2008). Changes in fecal pellet characteristics with depth as indicators of zooplankton repackaging of particles in the mesopelagic zone of the subtropical and subarctic North Pacific Ocean. *Deep Sea Res. II* 55, 1636–1647. doi: 10.1016/j.dsr2.2008.04.019

Wilson, S. E., Steinberg, D. K., Chu, F. L. E., and Bishop, J. K. B. (2010). Feeding ecology of mesopelagic zooplankton of the subtropical and subarctic North Pacific Ocean determined with fatty acid biomarkers. *Deep Sea Res. I* 57, 1278–1294. doi: 10.1016/j.dsr.2010.07.005

Wishner, K. F., Outram, D. M., Seibel, B. A., Daly, K. L., and Williams, R. L. (2013). Zooplankton in the eastern tropical north pacific: boundary effects of oxygen minimum zone expansion. *Deep Sea Res. Part I Oceanogr. Res. Pap.* 79, 122–140. doi: 10.1016/j.dsr.2013.05.012

Yoon, W. D., Kim, S. K., and Han, K. N. (2001). Morphology and sinking velocities of fecal pellets of copepod, molluscan, euphausiid, and salp taxa in the northeastern tropical Atlantic. *Mar. Biol.* 139, 923–928. doi: 10.1007/s002270100630

Conflict of Interest Statement: The authors declare that the research was conducted in the absence of any commercial or financial relationships that could be construed as a potential conflict of interest.